

# Shell evolution in neutron-rich carbon isotopes: Unexpected enhanced role of neutron-neutron correlation

C.X. Yuan<sup>a</sup>, C. Qi<sup>a,b</sup>, F.R. Xu<sup>a,c,\*</sup>

<sup>a</sup>State Key Laboratory of Nuclear Physics and Technology, School of Physics, Peking University, Beijing 100871, China

<sup>b</sup>KTH (Royal Institute of Technology), Alba Nova University Center, SE-10691 Stockholm, Sweden

<sup>c</sup>Center for Theoretical Nuclear Physics, National Laboratory for Heavy Ion Physics, Lanzhou 730000, China

---

## Abstract

Full shell-model diagonalization has been performed to study the structure of neutron-rich nuclei around  $^{20}\text{C}$ . We investigate in detail the roles played by the different monopole components of the effective interaction in the evolution of the  $N = 14$  shell in C, N and O isotopes. It is found that the relevant neutron-neutron monopole terms,  $V_{d_{5/2}d_{5/2}}^{nn}$  and  $V_{s_{1/2}s_{1/2}}^{nn}$ , contribute significantly to the reduction of the  $N = 14$  shell gap in C and N isotopes in comparison with that in O isotopes. The origin of this unexpectedly large effect, which is comparable with (sometimes even larger than) that caused by the proton-neutron interaction, is related to the enhanced configuration mixing in those nuclei due to many-body correlations. Such a scheme is also supported by the large  $B(E2)$  value in the nucleus  $^{20}\text{C}$  which has been measured recently.

**Keywords:** shell model, shell evolution,  $N = 14$  shell, carbon isotopes

---

## 1. Introduction

The study of neutron-rich nuclei with unusually large  $N/Z$  ratios is challenging the conventional view of nuclear structure [1, 2]. It is established that, when going from the  $\beta$ -stability line to drip line, the shell structure evolves and new magic numbers may emerge due to the dynamic effects of the nucleon-nucleon interaction. The influence of the proton-neutron interaction and its higher order term (namely the tensor force) has been extensively analyzed in recent publications [1, 3–8]. One may expect that other components of the nucleon-nucleon interaction contribute also to the shell evolution. However, this issue has not been much covered, which may be related to the fact that the isoscalar channel of the effective interaction is usually much stronger than the isovector part. In Ref. [9], it was found that a modification for the isovector  $T = 1$  channel of the monopole interaction is needed to reproduce the energies and electromagnetic transition properties of low-lying states in nuclei around  $^{17}\text{C}$ .

In this paper we analyze in detail contributions from the different terms of monopole interaction to the evolution of shell structure. In particular, we will show that the neutron-neutron monopole interaction can have significant effect on the evolution of  $N = 14$  shell in carbon isotopes. The rapid decrease of the  $E(2_1^+)$  in  $N = 14$  isotones indicates that the  $N = 14$  shell gap

---

\*Corresponding author at: School of Physics, Peking University, Beijing 100871, China

Email address: frxu@pku.edu.cn (F.R. Xu)

Preprint submitted to Elsevier

November 5, 2018

existing in oxygen isotopes erodes in nitrogen and carbon isotopes [1, 10–14]. At  $N = 14$ , the  $B(E2)$  value measured through the lifetime of the  $2_1^+$  state in  $^{20}\text{C}$  [15] is much larger than the values in  $^{16,18}\text{C}$  [16, 17] and  $^{22}\text{O}$  [18] while an inelastic scattering measurement presents a much smaller  $B(E2)$  value in  $^{20}\text{C}$  [19]. In this paper, we will also analyze  $E2$  transition properties in neutron-rich carbon isotopes from the viewpoint of collectivity.

In Sec. 2 we briefly introduce the theoretical framework. The influence of different monopole terms of the effective interaction on the evolution of the  $N = 14$  shell is discussed in Sec. 3.1. In Sec. 3.2 we analyze  $E2$  decay properties of the nuclei  $^{16,18,20}\text{C}$ . The calculations are summarized in Sec. 4.

## 2. Theoretical framework

The model space we choose contains  $p$  and  $sd$  shells [20]. To facilitate the calculation, we restrict the maximum number of two for nucleons that can be excited from  $p$  to  $sd$  shell. This truncation is denoted as  $2\hbar\omega$  space as usual. It should be mentioned that the full  $2\hbar\omega$  space should also include contributions such as the excitation of one nucleon from the  $p$  shell to the  $fp$  shell or from the  $0s$  shell to the  $sd$  shell. Such configurations are neglected in the present study, since they do not show any significant influence on the structure of nuclei of concern. Similarly, in the present work, the  $0\hbar\omega$  truncation implies that no nucleon is excited from the  $p$  shell to the  $sd$  shell. The well-established WBT [21] and MK [22] effective Hamiltonians are used. The WBT interaction is constructed based on the USD [23] interaction. The  $p$ -shell and  $psd$ -cross-shell matrices in WBT are determined by fitting experimental data. The  $sd$ ,  $p$ ,  $psd$  and  $ppsd$  parts in the MK interaction are taken from the PW interaction [24], CK interaction [25], MK potential [22] and Kuo-Brown G matrix [26], respectively. Calculations are carried out with a newly-established parallel shell-model code described in Ref. [27].

In  $2\hbar\omega$  calculations, one has to remove the spurious states which are caused by the center-of-mass motion. As suggested in Ref. [28], the shell model Hamiltonian  $H$  is modified to be  $H' = H + \beta H_{c.m.}$ , where  $H_{c.m.}$  is the center-of-mass Hamiltonian. One can separate the low-lying states from the spurious states by taking a large positive  $\beta$  value, which can move the center-of-mass excitations to high excitation energies. We take  $\beta = 100$  MeV in the present work, which is used in some previous works in this region [29–31].

The effective single-particle energy (ESPE) [32], describes in a simple manner the evolution of shell structure within the shell model framework [1, 3–6, 8]. The ESPE of a given  $j$  orbit is written as [8, 32]

$$\varepsilon_j = \varepsilon_j^{\text{core}} + \sum_{j'} V_{jj'} \langle \psi | \widehat{N}_{j'} | \psi \rangle, \quad (1)$$

where  $\varepsilon_j^{\text{core}}$  is the single-particle energy with respect to the core,  $\langle \psi | \widehat{N}_{j'} | \psi \rangle$  is the occupancy of nucleons in the  $j'$  orbit and  $V_{jj'}$  is the monopole interaction [33]. As in Ref. [8], one has

$$V_{jj',T} = \sum_J \left[ 1 - (-1)^{(2j-J-T+1)} \delta(jj') \right] \frac{(2J+1)}{(2j+1)(2j'+1)} \langle jj' | V | jj' \rangle_{JT}, \quad (2)$$

where  $\langle jj' | V | jj' \rangle_{JT}$  is the two-body matrix element and  $J$  and  $T$  are the angular momentum and the isospin of the corresponding two-particle state, respectively. To explore the influence of configuration mixing on the ESPE, we will adopt the occupancy in Eq. (1) obtained from the full shell-model diagonalization.

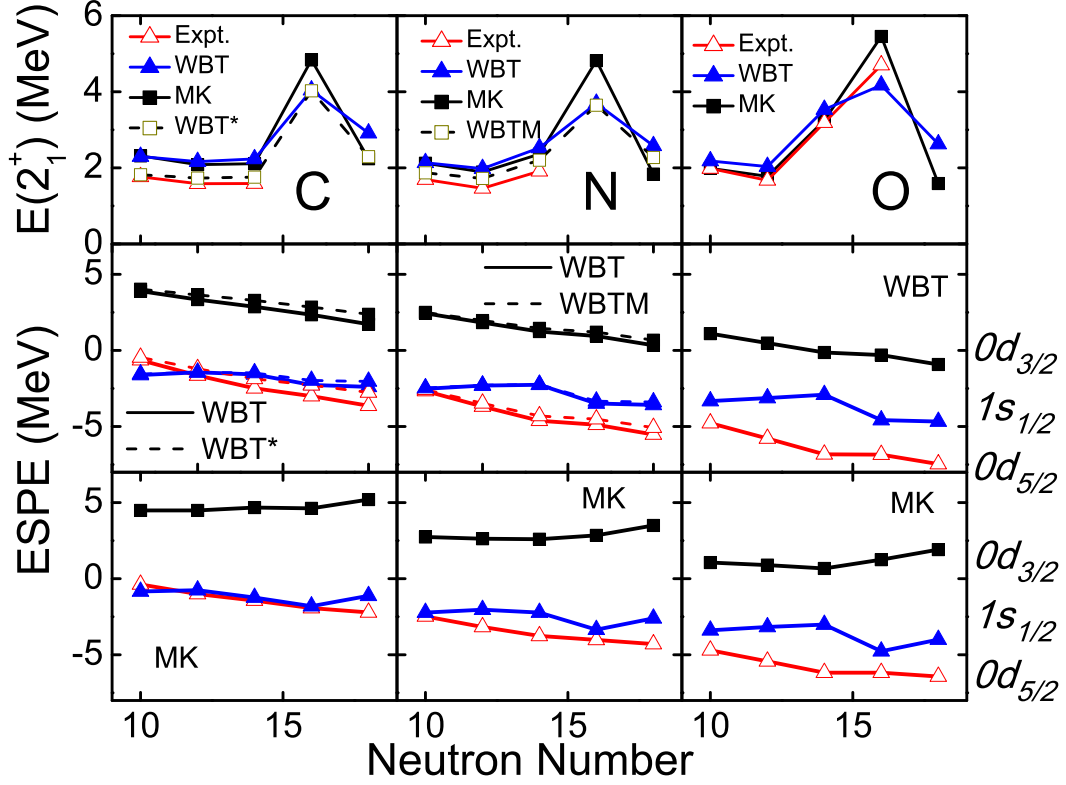


Figure 1: Calculated  $E(2_1^+)$  and ESPEs in even-neutron C, N and O isotopes. In N isotopes, the effective  $E(2_1^+)$  are deduced from the  $2J + 1$  weighted average of  $E(3/2_1^+)$  and  $E(5/2_1^+)$  [12]. Experimental data are from Refs. [10–12, 18, 35].

### 3. Calculations and discussions

#### 3.1. $N=14$ shell closure

In the independent particle model, the last neutrons in  $^{16}\text{C}$ ,  $^{18}\text{C}$  and  $^{20}\text{C}$  should occupy the  $\nu 0d_{5/2}$  orbit as in O isotopes. However, the ground state and the first excited state of  $^{15}\text{C}$  are  $1/2^+$  and  $5/2^+$  states, respectively, which indicates that the  $\nu 1s_{1/2}$  and  $\nu 0d_{5/2}$  orbits are inverse in  $^{15}\text{C}$  with respect to  $^{17}\text{O}$ . As noted in Ref. [34],  $^{16}\text{C}$  shows a strong  $(\nu 1s_{1/2})^2$  configuration. The rapid decrease of  $E(2_1^+)$  in  $N = 14$  isotones from O to C [10–12] also indicates that shell structures in O and C isotopes are different.

In order to study the structure difference between O and C isotopes, firstly we present  $E(2_1^+)$  and ESPEs in the even-neutron C, N and O isotopes, as shown in Fig. 1. For N isotopes, the energies are effective  $E(2_1^+)$  which are deduced from the  $2J + 1$  weighted average of  $E(3/2_1^+)$  and  $E(5/2_1^+)$  [12]. It is seen that the calculated  $E(2_1^+)$  values with WBT and MK interactions are systematically larger than experimental values in C and N isotopes. It has been pointed out that a reduction of  $V^m$  in the  $sd$  part of WBT can improve the results [11, 12]. For such an improvement, the modified versions of WBT have been suggested by multiplying the  $sd$  part of

$V^{nn}$  in WBT by a factor of 0.75 for C isotopes (named WBT\* [11]) and 0.875 for N isotopes (named WBTM [12]). We can see that the  $E(2_1^+)$  calculations are improved with WBT\* for C isotopes and WBTM for N isotopes, shown in Fig. 1. From  $^{18}\text{O}$  to  $^{16}\text{C}$ , the quenching of  $V^{nn}$  is explained via the core polarization effect [36]. In Fig. 1, we do not show the  $2\hbar\omega$  results, since they are very similar to the  $0\hbar\omega$  calculations. Both the energy and the  $\nu 0d_{5/2} - \nu 1s_{1/2}$  gap in N isotopes are almost in the middle of those in C and O isotopes.

In C isotopes, the calculated energy gap between  $\nu 1s_{1/2}$  and  $\nu 0d_{5/2}$  orbits is much smaller than what is shown in Ref. [11]. By calculating ESPEs with shell-model occupancy, the correlation effect is approximately included. So the ESPEs are different from those calculated with simple occupancy like assuming six neutrons all occupying  $\nu 0d_{5/2}$  orbits in  $^{20}\text{C}$  and  $^{22}\text{O}$ . The WBT\* and WBTM give smaller  $\nu 0d_{5/2} - \nu 1s_{1/2}$  gaps for C and N isotopes than those by WBT.

The role that each interaction plays in evolution of  $N = 14$  shell can be investigated based on present ESPEs. The energy gap between  $\nu 1s_{1/2}$  and  $\nu 0d_{5/2}$  is written as

$$\Delta\epsilon_{N=14} = \epsilon_{\nu 1s_{1/2}} - \epsilon_{\nu 0d_{5/2}}. \quad (3)$$

The difference between  $^{20}\text{C}$  and  $^{22}\text{O}$  is written as

$$\begin{aligned} \Delta\epsilon_{N=14}(^{22}\text{O}-^{20}\text{C}) &= \Delta\epsilon_{N=14}(^{22}\text{O}) - \Delta\epsilon_{N=14}(^{20}\text{C}) \\ &= [\epsilon_{\nu 1s_{1/2}}(^{22}\text{O}) - \epsilon_{\nu 1s_{1/2}}(^{20}\text{C})] - [\epsilon_{\nu 0d_{5/2}}(^{22}\text{O}) - \epsilon_{\nu 0d_{5/2}}(^{20}\text{C})] \\ &= \sum_j [\langle \nu 1s_{1/2} j' | V | \nu 1s_{1/2} j' \rangle_{JT} - \langle \nu 0d_{5/2} j' | V | \nu 0d_{5/2} j' \rangle_{JT}] \times \\ &\quad [N_j(^{22}\text{O}) - N_j(^{20}\text{C})]. \end{aligned} \quad (4)$$

The first part is the monopole interaction between the  $j'$ -th orbit and  $\nu 1s_{1/2}$  ( $\nu 0d_{5/2}$ ) orbit, while the second part is the difference of occupancy on  $j'$ -th orbit between  $^{22}\text{O}$  and  $^{20}\text{C}$ . Besides two  $0p_{1/2}$  protons, the numbers of protons and neutrons on other orbits are also different between  $^{22}\text{O}$  and  $^{20}\text{C}$ . The contribution from each term of the monopole interaction can be analyzed by Eq. (4). There are totally 20 terms of the monopole interaction which contribute in  $2\hbar\omega$  calculation. In  $0\hbar\omega$  calculation, the number of the terms reduces to 10 because no protons are in  $sd$  shell and neutrons in  $p$  shell are fully occupied in  $^{22}\text{O}$  and  $^{20}\text{C}$ .

Fig. 2 presents  $\Delta\epsilon_{N=14}(^{22}\text{O}-^{21}\text{N})$  and  $\Delta\epsilon_{N=14}(^{22}\text{O}-^{20}\text{C})$ , respectively. It is seen that the proton-neutron interaction,  $V_{p_{1/2}d_{5/2}}^{pn} - V_{p_{1/2}s_{1/2}}^{pn}$ , has large contribution to  $\Delta\epsilon_{N=14}$  as discussed in Ref. [11]. The two terms,  $V_{d_{5/2}d_{5/2}}^{nn}$  and  $V_{s_{1/2}s_{1/2}}^{nn}$ , have also significant contributions to  $\Delta\epsilon_{N=14}$ . In  $2\hbar\omega$  calculation, the influence of other 16 terms is small. When removing two protons from  $^{22}\text{O}$ , the proton-neutron interaction reduces the  $N = 14$  gap and enlarges the mixing between  $\nu 1s_{1/2}$  and  $\nu 0d_{5/2}$  orbits. At the same time, the neutron-neutron interaction contributes to the shell evolution because the neutrons in  $\nu 1s_{1/2}$  and  $\nu 0d_{5/2}$  orbits rearrange as a result of correlation effect from shell-model diagonalization. Although the ESPEs do not entirely include the correlation effect because the multipole interaction is not taken into account, we can approximately study the role of neutron-neutron correlation in shell evolution by applying occupancy obtained from full shell-model diagonalization to Eq. (1). The attractive neutron-neutron interactions are mostly due to the attractive singlet-even (SE) channel of the central force [8]. Specially,  $V_{s_{1/2}s_{1/2}}^{nn}$  is completely from this channel.

The study of shell evolution extends our understanding of nucleon-nucleon interaction, especially the tensor force [1, 3–8]. From a general view of shell evolution, when proton (neutron) number changes in isotones (isotopes), the neutron (proton) shell structure evolves due to the

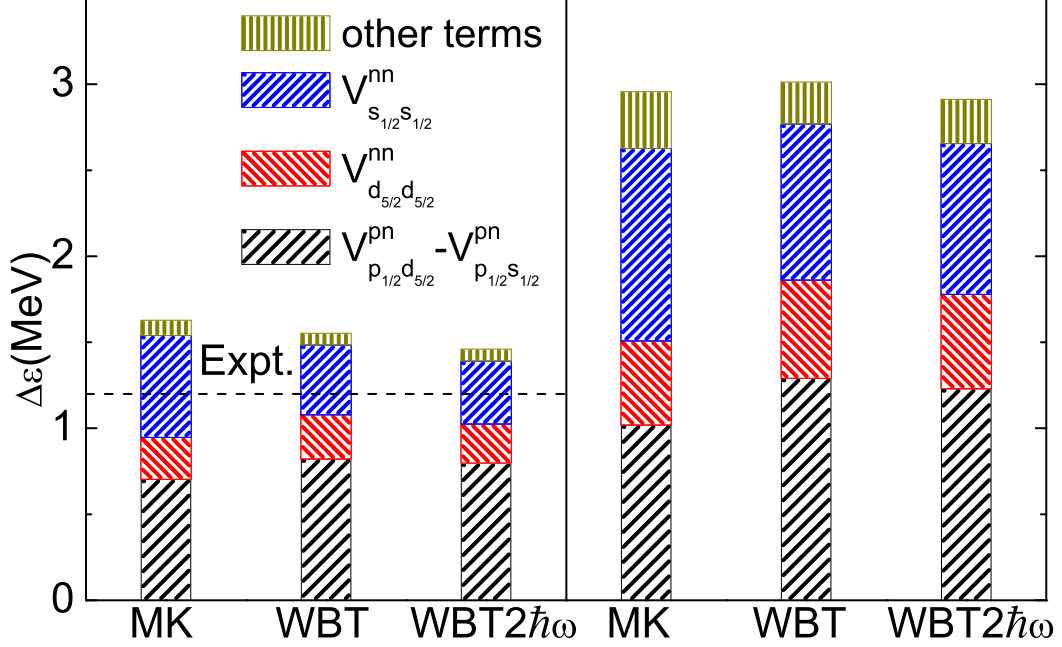


Figure 2: Contribution of each interaction in  $N = 14$  gap difference between  $^{22}\text{O}$  and  $^{21}\text{N}$  (left panel),  $^{22}\text{O}$  and  $^{20}\text{C}$  (right panel). The dashed line is for the value obtained from observed levels in  $^{22}\text{O}$  and  $^{21}\text{N}$  [12]. The  $2\hbar\omega$  calculations are indicated, otherwise  $0\hbar\omega$  calculations.

proton-neutron interaction. Here we present a detailed investigation on  $N = 14$  shell evolution to point out that the role played by the proton-neutron interaction in shell evolution can be “enhanced” by the attractive neutron-neutron interaction due to the many-body correlations. It is important to notice this “enhancement” if one wants to study the nuclear force from shell evolution. It is interesting to investigate the contribution of  $V_{jj}^{pp}$  and  $V_{jj}^{nn}$  in other cases of shell evolution in order to gain a complete understanding of how nuclear force drives the shell evolution. The  $N = 16$  shell existed in O isotopes will dramatically shrink in Si isotopes [3]. We adopt the similar method which we use in the study of  $N = 14$  shell for a detailed investigation of the  $N = 16$  shell evolution from  $^{24}\text{O}$  to  $^{30}\text{Si}$ . The result shows that, besides the proton-neutron interaction which was discussed in Ref. [3], the neutron-neutron interactions,  $V_{d_{3/2}d_{3/2}}^{nn}$  and  $V_{s_{1/2}s_{1/2}}^{nn}$ , contribute to the  $N = 16$  shell evolution from  $^{24}\text{O}$  to  $^{30}\text{Si}$ . Because of the limitation of calculation, it is hard to perform full shell-model diagonalization to study shell evolution in heavier regions, such as that in  $N = 51$  isotones which was discussed in Refs. [4, 5]. One may expect that more information from shell evolution can be gained through full shell-model diagonalization in heavier regions in the future.

### 3.2. $E2$ decay properties

Existing shell-model interactions reproduce well the observed  $B(E2)$  values for carbon isotopes [15, 37] including the large  $B(E2)$  value in  $^{20}\text{C}$ . In shell model, the  $B(E2)$  is calculated

Table 1: Calculated  $E2$  transition matrix elements and  $B(E2)$  values for even-even  $^{16-20}\text{C}$ . The SFO and SFO-tls calculations [37] are given for comparison.

	$A_p$ (fm)	$A_n$ (fm)	$B(E2)$ ( $e^4 fm^2$ )
$^{16}\text{C}$			
MK- $0\hbar\omega$	1.97	8.96	27.52
WBT- $0\hbar\omega$	1.27	9.39	20.88
WBT- $2\hbar\omega$	1.12	9.40	19.40
WBT*- $0\hbar\omega$	1.16	9.31	19.55
SFO	1.20	8.27	17.00
SFO-tls	1.38	8.06	18.20
Expt.			$13.0 \pm 1.0 \pm 3.5$ [17] $20.8 \pm 3.7$ [16]
$^{18}\text{C}$			
MK- $0\hbar\omega$	2.25	11.22	30.55
WBT- $0\hbar\omega$	1.77	11.16	24.74
WBT- $2\hbar\omega$	1.78	11.15	24.89
WBT*- $0\hbar\omega$	1.78	11.08	24.69
SFO	1.58	9.87	19.50
SFO-tls	1.60	9.69	19.90
Expt.			$21.5 \pm 1.0 \pm 5.0$ [17]
$^{20}\text{C}$			
MK- $0\hbar\omega$	3.64	11.82	42.19
WBT- $0\hbar\omega$	3.07	11.50	33.85
WBT- $2\hbar\omega$	3.00	11.32	32.43
WBT*- $0\hbar\omega$	2.96	11.30	31.95
Expt.			$37.5^{+15.0+5.0}_{-8.5-2.0}$ [15]

by

$$B(E2, j_i \rightarrow j_f) = \frac{1}{2j_i + 1} [e_p^{eff} A_p + e_n^{eff} A_n]^2, \quad (5)$$

where  $j_i$  and  $j_f$  are the angular moments of the initial and final states of the  $E2$  transition.  $A_p$  and  $A_n$  are proton and neutron  $E2$  transition matrix elements, respectively. In Table 1, we present  $A_p$ ,  $A_n$  and  $B(E2)$  values for even-even  $^{16-20}\text{C}$ . In the calculations, the oscillator parameter of  $\hbar\omega = 45A^{-1/3} - 25A^{-2/3}$  is employed. An approximate  $1/A$ -dependent effective charge is used [39]. For  $^{16-20}\text{C}$ , the effective charges are  $e_p^{eff}(e_n^{eff}) = 1.16(0.33), 1.11(0.27), 1.07(0.22)$ , respectively [39]. It is seen that the  $A_p$  increases significantly from  $^{16}\text{C}$  to  $^{20}\text{C}$ . Its contribution in  $B(E2)$  values is multiplied by  $e_p^{eff}$ . Thus the  $B(E2)$  value in  $^{20}\text{C}$  is much larger than those in  $^{16}\text{C}$  and  $^{18}\text{C}$ . As discussed in Refs. [15, 37], the reduction in the  $\pi 0p_{1/2} - \pi 0p_{3/2}$  gap from  $^{16}\text{C}$  to  $^{20}\text{C}$  would be one reason why the proton excitation probability and the  $B(E2)$  value increase from  $^{16}\text{C}$  to  $^{20}\text{C}$ .

The large  $B(E2)$  value in  $^{20}\text{C}$  can also be explained from the view of collectivity. In our previous work, we claimed that  $^{20}\text{C}$  may have large quadrupole deformation [38]. The intrinsic quadrupole moment  $Q_0(s)$  of the  $2_1^+$  state can be deduced from the spectroscopic quadrupole moment  $Q_{spec}$ . If the  $2_1^+$  state is a rotational deformed state, the intrinsic quadrupole moment

Table 2: Calculated intrinsic quadrupole moments  $Q_0(s)$  (from spectroscopic property) and  $|Q_0(t)|$  (from  $E2$  transition), and the ratio  $|Q_0(s)/Q_0(t)|$ . The experimental  $|Q_0(t)|$  are deduced from the observed  $B(E2)$  values [15–17].

	$Q_0(s)(fm^2)$	$ Q_0(t) (fm^2)$	$ Q_0(s)/Q_0(t) $
$^{16}\text{C}$			
MK- $0\hbar\omega$	10.07	16.63	0.61
WBT- $0\hbar\omega$	13.25	14.48	0.91
WBT- $2\hbar\omega$	13.93	13.96	1.00
WBT*- $0\hbar\omega$	13.53	14.02	0.97
Expt.		$11.43 \pm 1.98$ [17]	
		$14.44 \pm 1.27$ [16]	
$^{18}\text{C}$			
MK- $0\hbar\omega$	11.02	17.52	0.63
WBT- $0\hbar\omega$	11.19	15.77	0.71
WBT- $2\hbar\omega$	8.72	15.81	0.55
WBT*- $0\hbar\omega$	9.21	15.75	0.58
Expt.		$14.70 \pm 2.05$ [17]	
$^{20}\text{C}$			
MK- $0\hbar\omega$	-20.14	20.59	0.98
WBT- $0\hbar\omega$	-18.36	18.44	1.00
WBT- $2\hbar\omega$	-17.55	18.05	0.97
WBT*- $0\hbar\omega$	-17.44	17.92	0.97
Expt.		$19.41^{+5.18}_{-2.72}$ [15]	

(written as  $Q_0(t)$ ) can also be deduced from the  $B(E2; 2_1^+ \rightarrow 0_1^+)$  value of the  $E2$  transition. In the case of a good deformed rotor, these two definitions of the intrinsic quadrupole moments should give the similar values. One has

$$Q_0(s) = \frac{(J+1)(2J+3)}{3K^2 - J(J+1)} Q_{spec}(J), \quad (K \neq 1), \quad (6)$$

and

$$B(E2; J \rightarrow J-2) = \frac{5}{16\pi} e^2 | \langle JK20 | (J-2)K \rangle |^2 Q_0(t)^2, \quad (K \neq 1/2, 1). \quad (7)$$

In our case, we have  $K = 0$  and  $J = 2$ . The values of  $B(E2)$  and  $Q_{spec}$  can be calculated in shell model. Table 2 lists the intrinsic quadrupole moments for  $^{16}\text{C}$ ,  $^{18}\text{C}$  and  $^{20}\text{C}$ , and the ratios between  $Q_0(s)$  and  $Q_0(t)$ .

It is seen that  $Q_0(s)$  and  $Q_0(t)$  are almost the same in  $^{20}\text{C}$ , which, associated with a negative quadrupole moment, would indicate that  $^{20}\text{C}$  may have an oblate deformed structure, and thus the large  $B(E2)$  value in  $^{20}\text{C}$  might be understood with a consideration of the deformed collectivity. It may be of interest to understand why such collectivity is found in a nucleus as light as  $^{20}\text{C}$ . The six valence neutrons have strong configuration mixing due to the disappearance of the  $N = 14$  shell, and, due to the reduction of the proton  $0p_{1/2} - 0p_{3/2}$  gap in  $^{20}\text{C}$ , the probability of the proton

excitation to  $0p_{1/2}$  orbit increases, as discussed above. The strong mixing of configurations in both protons and neutrons would induce the enhanced collective property in  $^{20}\text{C}$ . The results from AMD [40] and deformed Skyrme-Hartree-Fock [39] have also shown an oblate deformation for  $^{20}\text{C}$ . Compared with  $^{20}\text{C}$ , the ratio between  $Q_0(s)$  and  $Q_0(t)$  in  $^{18}\text{C}$  is significantly less than the number of 1 in both WBT and MK calculations. Although we can not exclude other collective freedoms in  $^{18}\text{C}$  in the present study, the smaller  $Q_0(s)$  in  $^{18}\text{C}$  compared with  $^{20}\text{C}$  would indicate that the quadrupole deformation in  $^{18}\text{C}$  should be smaller than that in  $^{20}\text{C}$ . In case of  $^{16}\text{C}$ , the WBT and MK give rather different results. Calculations with the WBT interaction show that the nucleus  $^{16}\text{C}$  is well prolate deformed.

In the shell model where a spherical basis is used usually, the collectivity (or deformation) may be discussed in the language of configuration admixtures. In mean-field models, the collectivity (or deformation) can be discussed qualitatively by the filling of deformed orbits. The deformed Skyrme-Hartree-Fock calculation has been performed for  $^{17}\text{C}$  [41], giving coexisting prolate and oblate minima in each potential energy surface of the ground and lowly-excited states. It was predicted that the  $3/2^+$  g.s. has the lowest energy minimum at a prolate deformation while the first excited  $1/2^+$  state has the lowest minimum at an oblate shape [41]. The authors explained also that the observed hindered  $M1$  transition between the  $1/2^+$  and  $3/2^+$  states would be attributed to the shape difference of the two states [41]. If we look at the Nilsson diagram of single-particle orbits, the  $1/2[220]$  orbit of the  $0d_{5/2}$  shell has a prolate-driving force and  $5/2[202]$  has an oblate-driving force, while  $3/2[211]$  has a prolate-oblate competing force. For the  $3/2^+$  g.s. in  $^{17}\text{C}$ , the three valence neutrons outside the  $N = 8$  closed shell would have two on the  $1/2[220]$  orbit and one on  $3/2[211]$ , which would lead to a prolate deformation for the ground state. The first excited  $1/2^+$  state at the lowest energy should have two neutrons on  $5/2[202]$  and one on  $1/2[220]$ , which would make an oblate deformation. Back to the even-even C isotopes which we are investigating, the similar qualitative analyses of deformations may be made. The  $^{16,28,20}\text{C}$  isotopes should have coexisting prolate and oblate shapes, similar to  $^{17}\text{C}$ . The g.s. of  $^{16}\text{C}$  would favor a prolate shape with two valence neutrons occupying the prolate  $1/2[220]$  orbit.  $^{20}\text{C}$  would favor an oblate deformation with two neutrons on the oblate  $5/2[202]$  orbit, while  $^{18}\text{C}$  might be more shape-competitive between prolate and oblate deformations. These qualitative analyses are consistent with the shell-model calculations given in Table 2. However, it should be noted that the deformations of the carbon isotopes are rather soft, compared to heavy nuclei.

#### 4. Summary

In summary, the nuclei around  $^{20}\text{C}$  have been studied with shell model in  $0\hbar\omega$  and  $2\hbar\omega$  model spaces. The  $N = 14$  shell closure appears in O isotopes clearly, but vanishes in C isotopes [11, 12]. Besides the proton-neutron interaction which was discussed in Ref. [11], the neutron-neutron interactions,  $V_{d_{5/2}d_{5/2}}^{nn}$  and  $V_{s_{1/2}s_{1/2}}^{nn}$ , play also important role. When the  $N = 14$  shell gap is reduced, neutrons in the  $1s_{1/2}$  and  $0d_{5/2}$  orbits rearrange and the interactions  $V_{d_{5/2}d_{5/2}}^{nn}$  and  $V_{s_{1/2}s_{1/2}}^{nn}$  can have significant effects on the shell evolution. In  $2\hbar\omega$  calculation, other 16 terms of monopole interaction have very small contributions to the shell evolution. It would be useful to do systematic investigations on the contributions of  $V_{jj}^{pp}$  and  $V_{jj}^{nn}$  in order to understand the nuclear force from shell evolution.

As a special case of nuclei near the neutron drip line, we have analyzed the  $B(E2)$  value for  $^{20}\text{C}$  in which experimental data have been available. In Refs. [15, 37], it was pointed out that the large  $B(E2)$  in  $^{20}\text{C}$  is caused by the reduction of the proton  $0p_{1/2} - 0p_{3/2}$  gap, which leads



to a large proton transition matrix element. The present shell-model calculation gives the similar result. Usually, a large  $B(E2)$  value is connected with collectivity (or deformation). Therefore, we have made a further investigation of the problem. Our calculation gives a large quadrupole moment (or large  $B(E2)$ ) for  $^{20}\text{C}$ , indicating an increased collectivity (or deformation). In the shell-model language, the enhanced collectivity is caused by strong configuration mixings in both valence protons and neutrons.

## Acknowledgement

This work has been supported by the National Natural Science Foundation of China under Grant No. 10975006. CQ acknowledges the supports by the Swedish Research Council (VR) under grant Nos. 623-2009-7340 and 621-2010-4723 and the computational support provided by the Swedish National Infrastructure for Computing (SNIC) at PDC and NSC.

## References

- [1] O. Sorlin and M.-G. Porquet, *Prog. Part. Nucl. Phys.* 61 (2008) 602 .
- [2] R. V. F. Janssens, *Nature (London)* 459 (2009) 1069 .
- [3] T. Otsuka, R. Fujimoto, Y. Utsuno, B. A. Brown, M. Honma, and T. Mizusaki, *Phys. Rev. Lett.* 87 (2001) 082502.
- [4] T. Otsuka, T. Suzuki, R. Fujimoto, H. Grawe, and Y. Akaishi, *Phys. Rev. Lett.* 95 (2005) 232502.
- [5] T. Otsuka, T. Suzuki, M. Honma, Y. Utsuno, N. Tsunoda, K. Tsukiyama, and M. Hjorth-Jensen, *Phys. Rev. Lett.* 104 (2010) 012501.
- [6] N. A. Smirnova, B. Bally, K. Heyde, F. Nowacki and K. Sieja, *Phys. Lett. B* 686 (2010) 109.
- [7] Y. Utsuno, T. Otsuka, B. A. Brown, M. Honma, T. Mizusaki, N. Shimizu, *arXiv:1201.4077*.
- [8] A. Umeya and K. Muto, *Phys. Rev. C* 74 (2006) 034330.
- [9] T. Suzuki and T. Otsuka, *Int. J. Mod. Phys. E* 18 (2009) 1992.
- [10] M. Stanoiu, F. Azaiez, Zs. Dombrádi, O. Sorlin, B. A. Brown, M. Belleguic, D. Sohler, M. G. Saint Laurent, J. Lopez-Jimenez, Y. E. Penionzhkevich, G. Sletten, N. L. Achouri, J. C. Anglique, F. Becker, C. Borcea, C. Bourgeois, A. Bracco, J. M. Daugas, Z. Dlouhy, C. Donzau, J. Duprat, Zs. Fülöp, D. Guillemaud-Mueller, S. Grévy, F. Ibrahim, A. Kerek, A. Krasznahorkay, M. Lewitowicz, S. Leenhardt, S. Lukyanov, P. Mayet, S. Mandal, H. van der Marel, W. Mittig, J. Mrazek, F. Negoita, F. De Oliveira-Santos, Zs. Podolyák, F. Pougheon, M. G. Porquet, P. Roussel-Chomaz, H. Savajols, Y. Sobolev, C. Stodel, J. Timár, and A. Yamamoto, *Phys. Rev. C* 69 (2004) 034312.
- [11] M. Stanoiu, D. Sohler, O. Sorlin, F. Azaiez, Zs. Dombrádi, B. A. Brown, M. Belleguic, C. Borcea, C. Bourgeois, Z. Dlouhy, Z. Elekes, Zs. Fülöp, S. Grévy, D. Guillemaud-Mueller, F. Ibrahim, A. Kerek, A. Krasznahorkay, M. Lewitowicz, S. M. Lukyanov, S. Mandal, J. Mrázek, F. Negoita, Yu.-E. Penionzhkevich, Zs. Podolyák, P. Roussel-Chomaz, M. G. Saint-Laurent, H. Savajols, G. Sletten, J. Timár, C. Timis, and A. Yamamoto, *Phys. Rev. C* 78 (2008) 034315.
- [12] D. Sohler, M. Stanoiu, Zs. Dombrádi, F. Azaiez, B. A. Brown, M. G. Saint-Laurent, O. Sorlin, Yu.-E. Penionzhkevich, N. L. Achouri, J. C. Angélique, M. Belleguic, C. Borcea, C. Bourgeois, J. M. Daugas, F. De Oliveira-Santos, Z. Dlouhy, C. Donzau, J. Duprat, Z. Elekes, S. Grévy, D. Guillemaud-Mueller, F. Ibrahim, S. Leenhardt, M. Lewitowicz, M. J. Lopez-Jimenez, S. M. Lukyanov, W. Mittig, J. Mrázek, F. Negoita, Zs. Podolyák, M. G. Porquet, F. Pougheon, P. Roussel-Chomaz, H. Savajols, G. Sletten, Y. Sobolev, C. Stodel, and J. Timár, *Phys Rev. C* 77 (2008) 044303.
- [13] M. J. Strongman, A. Spyrou, C. R. Hoffman, T. Baumann, D. Bazin, J. Brown, P. A. DeYoung, J. E. Finck, N. Frank, S. Mosby, W. F. Rogers, G. F. Peaslee, W. A. Peters, A. Schiller, S. L. Tabor, and M. Thoennessen, *Phys Rev. C* 80 (2009) 021302(R).
- [14] Z. Elekes, Z. Vajta, Zs. Dombrádi, T. Aiba, N. Aoi, H. Baba, D. Bemmerer, Z. Fülöp, N. Iwasa, Á. Kiss, T. Kobayashi, Y. Kondo, T. Motobayashi, T. Nakabayashi, T. Nannichi, H. Sakurai, D. Sohler, S. Takeuchi, K. Tanaka, Y. Togano, K. Yamada, M. Yamaguchi, and K. Yoneda, *Phys Rev. C* 82 (2010) 027305.
- [15] M. Petri, P. Fallon, A. O. Macchiavelli, S. Paschalis, K. Starosta, T. Baugher, D. Bazin, L. Cartegni, R. M. Clark, H. L. Crawford, M. Cromaz, A. Dewald, A. Gade, G. F. Grinyer, S. Gros, M. Hackstein, H. B. Jeppesen, I. Y. Lee, S. McDaniel, D. Miller, M. M. Rajabali, A. Ratkiewicz, W. Rother, P. Voss, K. A. Walsh, D. Weisshaar, M. Wiedeking, and B. A. Brown, *Phys. Rev. Lett.* 107 (2011) 102501.

- [16] M. Wiedeking *et al.*, Phys. Rev. Lett. 100 (2008) 152501.
- [17] H. J. Ong, N. Imai, D. Suzuki, H. Iwasaki, H. Sakurai, T. K. Onishi, M. K. Suzuki, S. Ota, S. Takeuchi, T. Nakao, Y. Togano, Y. Kondo, N. Aoi, H. Baba, S. Bishop, Y. Ichikawa, M. Ishihara, T. Kubo, K. Kurita, T. Motobayashi, T. Nakamura, T. Okumura, and Y. Yanagisawa, Phys. Rev. C 78 (2008) 014308.
- [18] S. Raman, C. W. Nestor JR., and P. Tikkanen, At. Data Nucl. Data Tabl. 78 (2001) 1.
- [19] Z. Elekes, Zs. Dombrádi, T. Aiba, N. Aoi, H. Baba, D. Bemmerer, B.A. Brown, T. Furumoto, Z. Fülöp, N. Iwasa, Á. Kiss, T. Kobayashi, Y. Kondo, T. Motobayashi, T. Nakabayashi, T. Nannichi, Y. Sakuragi, H. Sakurai, D. Sohler, M. Takashina, S. Takeuchi, K. Tanaka, Y. Togano, K. Yamada, M. Yamaguchi, and K. Yoneda, Phys. Rev. C 79 (2009) 011302(R).
- [20] B. A. Brown, Prog. Part. Nucl. Phys. 47 (2001) 517.
- [21] E. K. Warburton and B. A. Brown, Phys. Rev. C 46 (1992) 923.
- [22] D. J. Millener and D. Kurath, Nucl. Phys. A 255 (1975) 315.
- [23] B. H. Wildenthal, Prog. Part. Nucl. Phys. 11 (1984) 5 ; B. A. Brown and B. H. Wildenthal, Annu. Rev. Nucl. Part. Sci. 38 (1988) 29.
- [24] B. M. Preedom and B. H. Wildenthal, Phys. Rev. C 6 (1972) 1633.
- [25] S. Cohen and D. Kurath, Nucl. Phys. 73 (1965) 1.
- [26] T. T. S. Kuo and G. E. Brown, Nucl. Phys. 85 (1966) 40 ; T. T. S. Kuo, Nucl. Phys. A 103 (1967) 71.
- [27] C. Qi and F. R. Xu, Chin. Phys. C 32(S2) (2008) 112.
- [28] D. H. Gloeckner and R. D. Lawson, Phys. Lett. B 53 (1974) 313.
- [29] A. Umeya, G. Kaneko, T. Haneda, and K. Muto, Phys. Rev. C 77 (2008) 044301.
- [30] H. L. Ma, B. G. Dong, and Y. L. Yan, Phys. Lett. B 688 (2010) 150.
- [31] Y. Utsuno and S. Chiba, Phys. Rev. C 83 (2011) 021301.
- [32] T. Otsuka, M. Honma, T. Mizusaki, N. Shimizu, and Y. Utsuno Prog. Part. Nucl. Phys. 47 (2001) 319.
- [33] R. K. Bansal and J. B. French, Phys. Lett. 11 (1964) 145.
- [34] T. Zheng, T. Yamaguchi, A. Ozawa, M. Chiba, R. Kanungo, T. Kato, K. Katori, K. Morimoto, T. Ohnishi, T. Suda, I. Tanihata, Y. Yamaguchi, A. Yoshida, K. Yoshida, H. Toki, and N. Nakajima, Nucl. Phys. A 709 (2002) 103.
- [35] C. R. Hoffman, T. Baumann, D. Bazin, J. Brown, G. Christian, D. H. Denby, P. A. DeYoung, J. E. Finck, N. Frank, J. Hinnefeld, S. Mosby, W. A. Peters, W. F. Rogers, A. Schiller, A. Spyrou, M. J. Scott, S. L. Tabor, M. Thoennessen, and P. Voss, Phys. Lett. B 672 (2009) 17.
- [36] K. Sieja and F. Nowacki, Nucl. Phys. A 857 (2011) 9.
- [37] T. Suzuki and T. Otsuka, Phys. Rev. C 78 (2008) 061301(R).
- [38] C. X. Yuan, C. Qi, and F. R. Xu, Chin. Phys. C 33(S1) (2009) 55.
- [39] H. Sagawa, X. R. Zhou, X. Z. Zhang, and T. Suzuki, Phys. Rev. C 70 (2004) 054316.
- [40] Y. Kanada-En'yo, Phys. Rev. C 71 (2005) 014310.
- [41] H. Sagawa, X. R. Zhou, T. Suzuki, and N. Yoshida, Phys. Rev. C 78 (2008) 041304(R).